Reynolds-number power-law scaling of differential molecular diffusion in turbulent nonpremixed combustion

Chao Han and Haifeng Wang*
School of Aeronautics and Astronautics, Purdue University, West Lafayette, Indiana 47907, USA

(Received 8 March 2018; published 10 October 2018)

A full understanding of differential molecular diffusion (DMD) in turbulent combustion has its theoretical significance for improving models of turbulent combustion. The scaling of the effect of DMD with respect to the Reynolds number in turbulent combustion is of particular interest for developing physically consistent modeling approaches for DMD. Such a scaling has so far been mostly studied in simple nonreacting flow problems, and a simple power-law scaling has been reported before. The applicability of the power-law scaling to turbulent combustion problems where the chemical reaction is expected to strongly couple with DMD has not been thoroughly studied. In this work, we aim to examine such a scaling by developing a statistical analysis of the dependence of DMD on the Reynolds number in turbulent nonpremixed combustion. Three Sandia temporally evolving planar jet nonpremixed CO/H_2 direct numerical simulation flames [E. R. Hawkes *et al.*, Proc. Combust. Inst. **31**, 1633 (2007)] are chosen as the target flames for the study. The Reynolds-number scaling based on a statistical analysis is reported, which is found to be statistically consistent with previous theoretical results in nonreacting problems. The results provide supportive evidence to the existence of a universal power-law scaling of the effect of DMD with respect to the Reynolds number in turbulent nonreacting and reacting flow problems. The results are also important for constraining the development of Reynolds-number-scaling consistent physical models for treating DMD in the modeling and simulations of multicomponent turbulent diffusion systems.

DOI: 10.1103/PhysRevFluids.3.103201

I. INTRODUCTION

Design improvement and optimization of combustion processes in combustion engines such as gasoline engines and gas turbines are needed regularly to meet more and more stringent design and regulatory requirements on emission. Computational and modeling tools of turbulent combustion have become vital for aiding the design and optimization of combustion processes. The success of computational and modeling tools highly relies on the accuracy of the models that are developed to describe the underlying physicochemical processes in combustion. It is an overarching issue to develop accurate and predictive models to improve the design of combustion configurations.

Turbulent combustion is a classic multiscale, multiphysical, and highly nonlinear phenomenon, involving many physicochemical processes such as fluid dynamics, turbulence, molecular diffusion, chemical kinetics, radiation, multiphase, heat transfer, and acoustics [1–3]. Among them, molecular diffusion in turbulent combustion is the main focus of this work. In a multicomponent gas-phase system like combustion, a phenomenon called differential molecular diffusion (DMD) [4,5] (or preferential molecular diffusion [6]) is encountered when the different components have different molecular diffusivities. The significance of DMD in turbulent combustion has been recognized for

*haifeng@purdue.edu

a while. In turbulent premixed flames, it has been demonstrated that DMD can strongly affect the turbulent flame speed [7], flame width [8], flame structures [9], flame instabilities [10], and local extinction [11]. In turbulent nonpremixed flames, it has also been shown that DMD can significantly influence flame structures [12], local extinction [13], flame stabilization [14], and flame ignition [15,16].

In the past modeling studies of turbulent combustion, the effect of DMD is often neglected, based on the assumption of negligible effect of molecular diffusion on scalar transport in high-Reynolds-number turbulent flows [1,3]. The incorporation of DMD into turbulent combustion models has emerged only recently. Kronenburg and Bilger [17,18] obtained equations including the DMD effect in the conditional moment closure (CMC) model and proposed an approach based on direct numerical simulation (DNS) to model the additional terms introduced by the incorporation of DMD. Reasonable results were demonstrated by incorporating DMD in CMC and more accurate NO formation rates were predicted in the near field of a turbulent jet flame. A similar work was reported in [19], where the CMC equations with the DMD effect for species and enthalpy were derived and the effect of nonunity Lewis numbers of species H and H_2 on the combustion fields was examined. In the transported probability density function (PDF) method [20], an approach to treat spatial DMD was presented by McDermott and Pope [21]. In this approach, the spatial molecular transport of scalars was modeled by a mean shift (MS) model in the composition space to replace the traditional random-walk model in the physical space [22], which is unable to treat DMD. Zhang and Wang [23] improved the MS model by developing a variance-consistent mean shift model to yield consistent transport of scalar variance. In the flamelet models [24], a consistent laminar flamelet equation with DMD was derived by Pitsch and Peters [25] and can be incorporated into flamelet models straightforwardly. However, this model tends to significantly overpredict the effect of DMD, especially at the downstream locations of a turbulent jet flame [26]. Wang [5] argued that this overprediction was due to the missing Reynolds-number dependence of DMD in the model. A class of consistent DMD flamelet models, called the linear differential diffusion model and the nonlinear differential diffusion model, was developed by Wang [5] to incorporate the effect of Reynolds number on DMD in the flamelet models.

Developing accurate models for DMD relies on an accurate understanding of the statistics of DMD. A critically important aspect of DMD in turbulent flow problems is the scaling of the effect of DMD with respect to the Reynolds number, which is the focus of this work. To study this scaling, we need to establish a quantification method for DMD and an appropriate definition of the Reynolds number.

The effect of DMD is commonly quantified by a parameter $z_{\alpha\beta}$ [4,5,12,27],

$$z_{\alpha\beta}(\mathbf{x}, t) = \xi_\alpha(\mathbf{x}, t) - \xi_\beta(\mathbf{x}, t), \tag{1}$$

$$\xi_\alpha(\mathbf{x}, t) = \frac{Y_\alpha(\mathbf{x}, t) - Y_{\alpha,\mathrm{ox}}}{Y_{\alpha,\mathrm{fu}} - Y_{\alpha,\mathrm{ox}}}, \tag{2}$$

where $\mathbf{x}$ is the physical space vector, t is time, Y_α is the mass fraction of element α, ξ_α is the mixture fraction defined based on the mass fractions of element α, Y_α, and the subscripts ox and fu denote the oxidizer boundary and the fuel boundary for a two-inlet nonpremixed combustion system, respectively. The moments of $z_{\alpha\beta}$ and ξ_α in turbulent flames can be readily obtained by performing Favre averaging, e.g., the mean $\tilde{z}_{\alpha\beta}(\mathbf{x}, t) = \widetilde{\xi}_\alpha(\mathbf{x}, t) - \widetilde{\xi}_\beta(\mathbf{x}, t)$ and the rms $z_{\alpha\beta,\mathrm{rms}}(\mathbf{x}, t) = (\widetilde{z^2_{\alpha\beta}} - \tilde{z}^2_{\alpha\beta})^{0.5}$.

Different definitions of the Reynolds number can be used to study the DMD scaling. One definition is based on a bulk Reynolds number

$$\mathrm{Re}_b = \frac{UL}{\nu}, \tag{3}$$

where U is a characteristic bulk velocity, L is a length scale, and ν is the kinematic viscosity. This Re_b number is a characteristic Reynolds number representing a whole turbulence field. A local turbulent Reynolds number can also be defined based on the turbulence integral scales to study the DMD scaling,

$$\mathrm{Re}_t = \frac{ul}{\nu}, \tag{4}$$

where the integral turbulent velocity scale is defined as $u = \sqrt{2k/3}$ and the turbulent integral length scale is defined as $l = \sqrt{2k^3/3}/\varepsilon$ [5]. Here k is the turbulent kinetic energy and ε is the turbulent kinetic energy dissipation rate. It is argued that the local turbulent Reynolds number is probably more appropriate for studying the DMD scaling since DMD is a small-scale local phenomenon.

Bilger and Dibble [4] suggested that $\tilde{z}_{\alpha\beta}$ and $z_{\alpha\beta,\mathrm{rms}}$ both follow a simple power-law scaling as Re_t^{-1} in turbulent flows. A different scaling of $z_{\alpha\beta,\mathrm{rms}} \sim \mathrm{Re}_t^{-0.25}$, however, was reported in [28–30] for nonreacting flows. The extensibility of this power-law scaling of $z_{\alpha\beta,\mathrm{rms}} \sim \mathrm{Re}_t^{-0.25}$ found in nonreacting problems to reacting problems remains to be validated. Han *et al.* [27] attempted a scaling analysis of DMD in a series of Sandia CO/H_2 DNS flames and found that the power-law scaling of $z_{\mathrm{HC,rms}}$ ranges between $\mathrm{Re}_b^{-0.04}$ and $\mathrm{Re}_b^{-0.57}$, where Re_b is used for the scaling study. There are also reports in the literature that do not support evident power-law scaling of DMD in turbulent nonpremixed flames (e.g., [31] for H_2/CO flames). This work further examines the scaling of DMD in turbulent nonpremixed flames with the goal to provide consistent results for the Reynolds-number scaling.

The theoretical scaling $\tilde{z}_{\alpha\beta} \sim \mathrm{Re}_t^{-1}$ and $z_{\alpha\beta,\mathrm{rms}} \sim \mathrm{Re}_t^{-0.25}$ can be readily explained. For the mean scalars, the molecular diffusion affects the scalar transport in turbulence only through the spatial molecular diffusion term, which is inversely proportional to the Reynolds number. This leads to the scaling of DMD in terms of the mean $\tilde{z}_{\alpha\beta}$ also inversely proportional to the Reynolds number. For the second-order moment, the molecular diffusion affects the transport in both the spatial molecular diffusion term and the dissipation term. The spatial molecular diffusion for the second-order moment is also inversely proportional to the Reynolds number, which also suggests the scaling of $z_{\alpha\beta,\mathrm{rms}} \sim \mathrm{Re}_t^{-1}$. Meanwhile, based on Kolmogorov's eddy cascading hypothesis and turbulent scalar spectrum [1,28,32], scalars dissipate at either the Batchelor scale [33] or the Oboukov-Corrsin scale [34] and the dissipation is found to be correlated to the reciprocal of the square root of the Reynolds number; as a result, the DMD effect through scalar dissipation is expected to have a Reynolds-number scaling of $z_{\alpha\beta,\mathrm{rms}} \sim \mathrm{Re}_t^{-0.25}$. Theoretically, the scaling of $z_{\alpha\beta,\mathrm{rms}} \sim \mathrm{Re}_t^{-1}$ is anticipated in the situation where the spatial molecular transport effect dominates the dissipation effect; the scaling of $z_{\alpha\beta,\mathrm{rms}} \sim \mathrm{Re}_t^{-0.25}$ is evident when the dissipation dominates. The latter case is general in real-life turbulence and hence the scaling $z_{\alpha\beta,\mathrm{rms}} \sim \mathrm{Re}_t^{-0.25}$ is generally expected. The simple Reynolds-number scaling of DMD has a solid physical basis for ideal turbulence. Its extensibility to real turbulence accompanied by chemical reaction remains to be confirmed. Once confirmed, the Reynolds-number scaling of DMD will be useful for guiding the development of consistent DMD models as well as for validating the consistency of existing models. Wang [5] incorporated the Reynolds-number dependence in the flamelet model for treating DMD and obtained excellent agreement of the flamelet predictions with the experimental measurements for the mean values $\tilde{z}_{\alpha\beta}$. The model consistency for the second-order moment of z, $z_{\alpha\beta,\mathrm{rms}}$, has not been examined and it is not clear what the right Reynolds-number scaling for the model to reproduce is.

This work is motivated by the incomplete knowledge of the Reynolds-number scaling of DMD in turbulent nonpremixed flames. The objective of the work is to develop a statistical analysis to gain a consistent Reynolds-number scaling of DMD in turbulent nonpremixed flames by analyzing three Sandia CO/H_2 DNS flames [35]. The rest of the paper is organized as follows. Section II examines the three Sandia CO/H_2 DNS flames. Section III presents a statistical analysis to obtain the Reynolds-number scaling of DMD in these flames. A summary is given in Sec. IV.

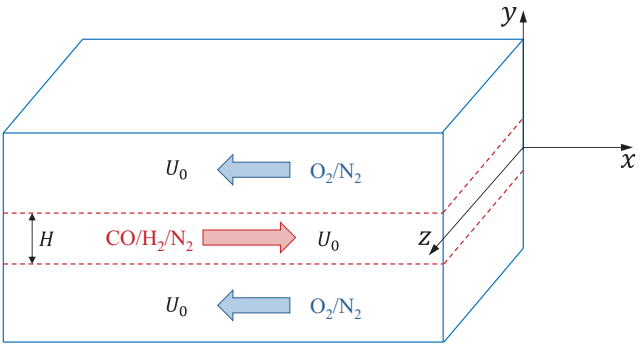

FIG. 1. Sketch of the Sandia temporally evolving jet CO/H_2 DNS flames [35].

II. DIFFERENTIAL MOLECULAR DIFFUSION IN SANDIA CO/H_2 DNS FLAMES

Three Sandia DNS flames are chosen as the target flames for the Reynolds-number-scaling analysis of DMD. The DNS flame conditions, the characterization of DMD in the flames, and some sample statistics of the flames are briefly summarized in this section.

A. Sandia CO/H_2 DNS flames

The flame configuration of the temporally evolving plane jet CO/H_2 DNS flames [35] is illustrated in Fig. 1. The fuel stream consisting of 50% CO, 10% H_2, and 40% N_2 by volume flows at the center and is surrounded by two counterflowing oxidizer streams with 25% O_2 and 75% N_2 by volume. The stoichiometric mixture fraction is 0.42 based on the Bilger definition [36]

$$\xi_{\text{Bilger}} = \frac{\left(\frac{2Y_C}{M_C} + \frac{Y_H}{2M_H} - \frac{Y_O}{M_O}\right) - \left(\frac{2Y_{C,ox}}{M_C} + \frac{Y_{H,ox}}{2M_H} - \frac{Y_{O,ox}}{M_O}\right)}{\left(\frac{2Y_{C,fu}}{M_C} + \frac{Y_{H,fu}}{2M_H} - \frac{Y_{O,fu}}{M_O}\right) - \left(\frac{2Y_{C,ox}}{M_C} + \frac{Y_{H,ox}}{2M_H} - \frac{Y_{O,ox}}{M_O}\right)}, \tag{5}$$

where M_α is the molecular weight for the element α. Three flow conditions are available, case L, case M, and case H, as summarized in Table I. In these flames, the initial fuel stream bulk velocity U_0 and the initial jet width H are adjusted to vary the bulk Reynolds number $\text{Re}_b = U_0 H/\nu$, while the flow timescale $t_0 = H/U_0$ is kept the same so that the Damköhler number $\text{Da} = \chi_{\text{ex}} t_0$ is the same ($\chi_{\text{ex}} = 2194\ \text{s}^{-1}$ is the extinction scalar dissipation rate limit in laminar opposed jet diffusion flames to represent the chemical timescale) [35]. The DNS domain size is $12H$ in the x direction, $14H$ in the y direction, and $8H$ in the z direction. The grid resolution is uniform with the grid size $0.0208H = 0.015$ mm, $0.0156H = 0.015$ mm, and $0.0139H = 0.019$ mm for cases L, M, and H, respectively. A periodic boundary condition is used in the x and z directions and a nonreflecting outflow boundary condition is used in the y direction. The compressible Navier-Stokes equations are solved with eighth-order explicit finite differencing in space and the fourth-order Runge-Kutta method in time. For more details about the DNS cases, the readers are referred to the original DNS reference [35]. The fixed Da of the three cases provides a set of flames with the effect of the

TABLE I. Operating conditions of the Sandia CO/H_2 DNS flames [35].

Parameter	Case L	Case M	Case H
H (mm)	0.72	0.96	1.37
U_0 (m/s)	72.5	97	138
$\text{Re}_b = U_0 H/\nu$	2510	4478	9079
$t_0 = H/U_0$ (ms)	0.01	0.01	0.01
Da	0.011	0.011	0.011

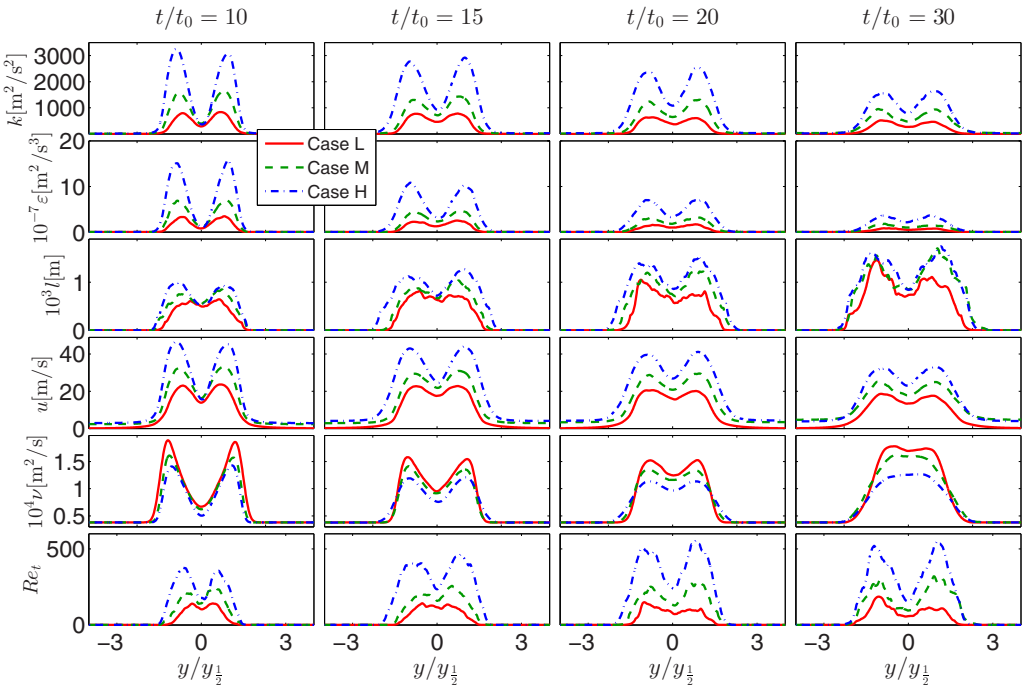

FIG. 2. Profiles of the turbulent kinetic energy k, the turbulence dissipation rate ε, the turbulence integral length scale l, the turbulence integral velocity scale u, the molecular viscosity ν, and the turbulent Reynolds number Re_t in the three Sandia CO/H_2 DNS flames [35] at the different times $t/t_0 = 10$, 15, 20, and 30 against $y/y_{1/2}$, where $y_{1/2}$ is the half-width of the mixing layer based on the profiles of $\tilde{\xi}_C$.

Reynolds number isolated so that the scaling of DMD with respect to the Reynolds number can be readily examined. The mixture-averaged diffusion model was used in the DNS to account for molecular diffusion. It has been shown that the mixture-averaged diffusion model is an adequate model for describing molecular diffusion in combustion [37] generally, and it is suitable for the current scaling study of the effect of DMD.

The turbulence characteristics of the DNS flames are shown in Fig. 2 in terms of the spatial profiles of the turbulent kinetic energy k, the turbulent kinetic energy dissipation rate ε, the integral length scale l, the integral velocity scale u, the kinematic viscosity ν, and the turbulent Reynolds number Re_t against $y/y_{1/2}$, where $y_{1/2}$ is the half-width of the mixing layer based on the profiles of $\tilde{\xi}_C$. The Favre-averaged statistics such as k and ε are obtained by averaging the DNS data in the spanwise direction z and the streamwise direction x. All quantities that are shown in the figure exhibit double peaks around the two flame fronts. The increase of the bulk Reynolds number Re_b from case L to case H leads to the increase of k, ε, l, and u. The kinematic viscosity ν decreases with the increase of the Reynolds number mainly because of the decrease of flame temperature due to the increased flame local extinction from case L to case H. The local turbulent Reynolds number Re_t increases with the increase of Re_b.

B. Characterization of DMD in the Sandia CO/H_2 DNS flames

The effect of DMD is commonly quantified by $z_{\alpha\beta}$, $\tilde{z}_{\alpha\beta}$, and $z_{\alpha\beta,\mathrm{rms}}$. Different element pairs in Eq. (1), α and β, can be used to examine DMD in these DNS flames. Han *et al.* [27] demonstrated that the element pair of hydrogen and carbon is representative to show the effect of DMD. In this work, we choose the elements H and C for examining the Reynolds-number scaling of DMD, i.e., in terms of $\tilde{z}_{\mathrm{HC}}$ and $z_{\mathrm{HC,rms}}$.

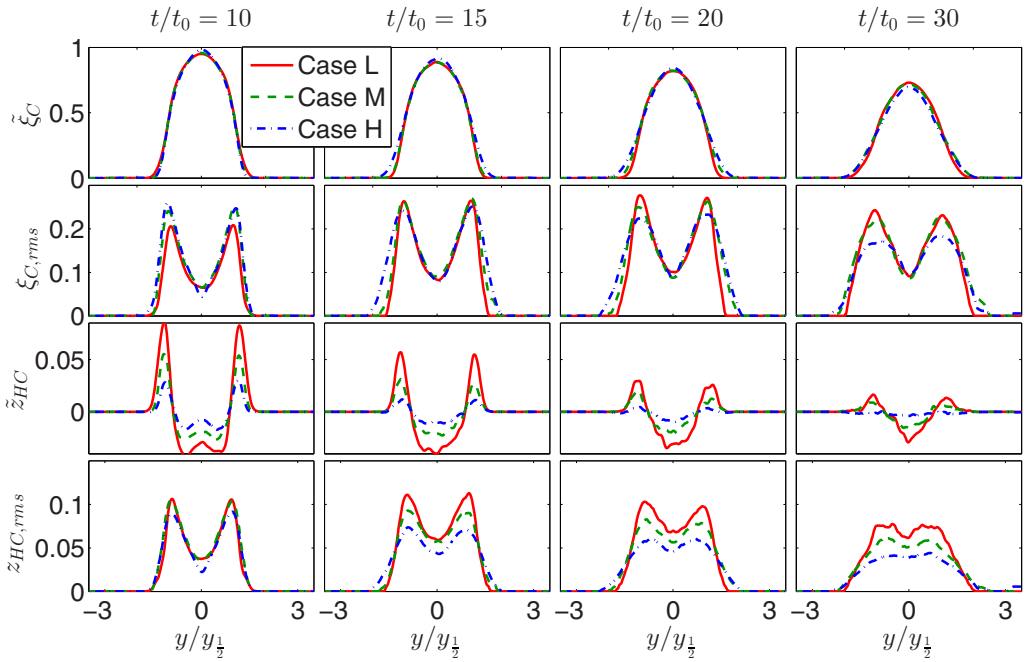

FIG. 3. Profiles of mean mixture fraction $\widetilde{\xi}_{\mathrm{C}}$, rms of mixture fraction $\xi_{\mathrm{C,\,rms}}$, mean $\tilde{z}_{\mathrm{HC}}$, and rms $z_{\mathrm{HC,rms}}$ against $y/y_{1/2}$ in the three Sandia CO/H_2 DNS flames at the different times $t/t_0 = 10$, 15, 20, and 30.

We first briefly examine the scalar statistics in the CO/H_2 DNS flames to provide an overview of the flames before we examine the scaling of DMD in Sec. III. Figure 3 shows the profiles of the mean mixture fraction $\widetilde{\xi}_{\mathrm{C}}$ (based on the element C), the rms of mixture fraction $\xi_{\mathrm{C,rms}}$, the mean $\tilde{z}_{\mathrm{HC}}$, and the rms $z_{\mathrm{HC,rms}}$ for the three CO/H_2 DNS flames (cases L, M, and H) at the different times $t/t_0 = 10$, 15, 20, and 30 against $y/y_{1/2}$. From the figure we can observe that the profiles of $\widetilde{\xi}_{\mathrm{C}}$ against $y/y_{1/2}$ are only slightly different in the different flames at the same t/t_0, which indicates a weak sensitivity of $\widetilde{\xi}_{\mathrm{C}}$ to Re_b in the three cases. The profiles of $\xi_{\mathrm{C,rms}}$ against $y/y_{1/2}$ in Fig. 3 are influenced by Re_b slightly. At $t/t_0 = 10$, the peak value of $\xi_{\mathrm{C,rms}}$ increases with the increase of Re_b from case L to case H, while at $t/t_0 \geqslant 15$, the peak value decreases with the increase of Re_b. The peak magnitudes of $\tilde{z}_{\mathrm{HC}}$ and $z_{\mathrm{HC,rms}}$ are on the order of 0.1, and with the increase of Re_b from case L to case H, both $\tilde{z}_{\mathrm{HC}}$ and $z_{\mathrm{HC,rms}}$ show the trend of decreasing, which is consistent with the theory that the effect of DMD decreases when the Reynolds number increases [4,5]. The purpose of this paper is to find the quantitative Reynolds-number scaling of the effect of DMD. From Fig. 3 we can also see that the value of $\tilde{z}_{\mathrm{HC}}$ is negative on the fuel side while it is positive near the oxidizer side, which is caused by the higher molecular diffusion rate of light molecules such as H_2 and H.

In summary, an overview of the Sandia CO/H_2 DNS flames and some selected statistical results in the flames are provided in this section. The dependence of DMD on the Reynolds number is qualitatively examined. In the following section we conduct an analysis to gain the quantitative Reynolds-number scaling of such a dependence.

III. SCALING ANALYSIS OF DIFFERENTIAL MOLECULAR DIFFUSION IN DNS FLAMES

A. Scaling analysis approach

We aim to gain a quantitative Reynolds-number scaling of DMD from the three CO/H_2 DNS flames. Similar analyses have been reported before, mostly in nonreacting problems. A unique

scaling of the mean $\tilde{z}_{\mathrm{HC}} \sim \mathrm{Re}_t^{-1}$ has been reported extensively (see, e.g., [4,27,28,38]). The scaling of the rms $z_{\mathrm{HC,rms}}$ has also been studied, but different scaling laws have been reported, e.g., $z_{\mathrm{HC,rms}} \sim \mathrm{Re}_t^{-1}$ [4] or $z_{\mathrm{HC,rms}} \sim \mathrm{Re}_t^{-0.25}$ [28–30] based on theoretical studies. As discussed in Sec. I, both scalings for $z_{\mathrm{HC,rms}}$ can be explained theoretically, but the latter is likely the dominant scaling in real turbulence problems. The scaling of DMD has seldom been examined in real flames. Han *et al.* [27] attempted the analysis and obtained a power-law scaling with the exponent that varies widely in the Sandia CO/H_2 DNS flames and hence produced inconsistent results with previous findings. It is not clear what the cause of this inconsistency is, and more work is needed to reconcile the different findings. This work serves as a significant extension of [27] with the goal to obtain more consistent and reliable scaling results of DMD against the Reynolds number in turbulent nonpremixed flames.

In [27], the scaling of DMD was examined based on $\tilde{z}_{\mathrm{HC}}(\mathbf{x}, t)$ and $z_{\mathrm{HC,rms}}(\mathbf{x}, t)$ against the bulk Reynolds number Re_b shown in Table I. There are two problems with their analysis. First, in addition to the dependence on the Reynolds number, $\tilde{z}_{\mathrm{HC}}$ and $z_{\mathrm{HC,rms}}$ have other dependences such as on the local chemical compositions and scalar dissipation rate. The additional dependence, which was not considered by Han *et al.* [27], can potentially interfere with the Reynolds-number scaling for $\tilde{z}_{\mathrm{HC}}$ and $z_{\mathrm{HC,rms}}$ and results in inconsistent results. Second, the Reynolds number used for the analysis by Han *et al.* [27] is the bulk Reynolds number Re_b as defined in Table I. Differential molecular diffusion is a small-scale local phenomenon, and using a bulk Re_b is unlikely a suitable choice for revealing the true scaling that strongly depends on local turbulence level. This work chooses the same DNS flames and seeks a more rigorous analysis to isolate the dependence of DMD on the Reynolds number through conditioning in order to provide more reliable and consistent scaling results.

In general, in turbulent nonpremixed flames, the statistics of z_{HC} such as $\tilde{z}_{\mathrm{HC}}$ and $z_{\mathrm{HC,rms}}$ depends on many parameters such as the statistics of the chemical compositions, Re_t, Da, and the Lewis number Le. In the Sandia CO/H_2 DNS flames, the fuel and oxidizer are fixed and hence Le is fixed among the three CO/H_2 DNS flames. The dimensionless number Da among the different flames is also fixed by design [35]. By employing the steady flamelet concept [24], i.e., the chemical composition variables are approximately related to $(\widetilde{\xi}_{\mathrm{C}}, \xi_{\mathrm{C,rms}}, \tilde{\chi}_{\mathrm{st}})$, where $\widetilde{\chi}_{\mathrm{st}}$ is the mean scalar dissipation rate at the stoichiometric condition, we can readily approximate $\tilde{z}_{\mathrm{HC}}$ and $z_{\mathrm{HC,rms}}$ as

$$\tilde{z}_{\mathrm{HC}} \approx \tilde{z}_{\mathrm{HC}}(\widetilde{\xi}_{\mathrm{C}}, \xi_{\mathrm{C,rms}}, \tilde{\chi}_{\mathrm{st}}, \mathrm{Re}_t), \tag{6}$$

$$z_{\mathrm{HC,rms}} \approx z_{\mathrm{HC,rms}}(\widetilde{\xi}_{\mathrm{C}}, \xi_{\mathrm{C,rms}}, \tilde{\chi}_{\mathrm{st}}, \mathrm{Re}_t), \tag{7}$$

where Re_t is added to the flamelet approximation to account for the dependence of DMD on it. In the following analysis, we examine the scaling of DMD by conditionally sampling the statistics $\tilde{z}_{\mathrm{HC}}(\mathbf{x}, t)$ and $z_{\mathrm{HC,rms}}(\mathbf{x}, t)$ in the three Sandia CO/H_2 flames with the same values of $\widetilde{\xi}_{\mathrm{C}}$, $\xi_{\mathrm{C,rms}}$, and $\widetilde{\chi}_{\mathrm{st}}$ so that the sole dependence on Re_t can be better revealed.

The DNS data used for this analysis contain the time history of the computed statistics (at about 250 sample time steps) by averaging in the spanwise direction z and the streamwise direction x. The data are conditionally sampled into the groups $\tilde{z}_{\mathrm{HC}}|_{\mathbf{C}}$ or $z_{\mathrm{HC,rms}}|_{\mathbf{C}}$ with the condition $\mathbf{C}$ defined as

$$\begin{aligned}\mathbf{C}(c_m, c_r, c_\chi) = &\{\widetilde{\xi}_{\mathrm{C}} : \widetilde{\xi}_{\mathrm{C}} \in [c_m(1-\epsilon_m), c_m(1+\epsilon_m)]\} \\ &\bigcap \{\xi_{\mathrm{C,rms}} : \xi_{\mathrm{C,rms}} \in [c_r(1-\epsilon_r), c_r(1+\epsilon_r)]\} \\ &\bigcap \{\widetilde{\chi}_{\mathrm{st}} : \log_{10}(\widetilde{\chi}_{\mathrm{st}}) \in [c_\chi(1-\epsilon_\chi), c_\chi(1+\epsilon_\chi)]\},\end{aligned} \tag{8}$$

where $\bigcap$ denotes intersection and c_m and ϵ_m are used to define the conditioning interval for the mean $\widetilde{\xi}_{\mathrm{C}}$, c_r and ϵ_r for $\xi_{\mathrm{C,rms}}$, and c_χ and ϵ_χ for $\widetilde{\chi}_{\mathrm{st}}$. The finite sampling intervals are used in order to have enough data points under the condition. Ideally, the interval needs to be as small as possible to ensure accurate sampling under a particular condition, while it also needs to be big enough to have enough samples in the interval. In this work $\epsilon_m = 5 \times 10^{-3}$, $\epsilon_r = 8 \times 10^{-4}$, and $\epsilon_\chi = 0.2$ are

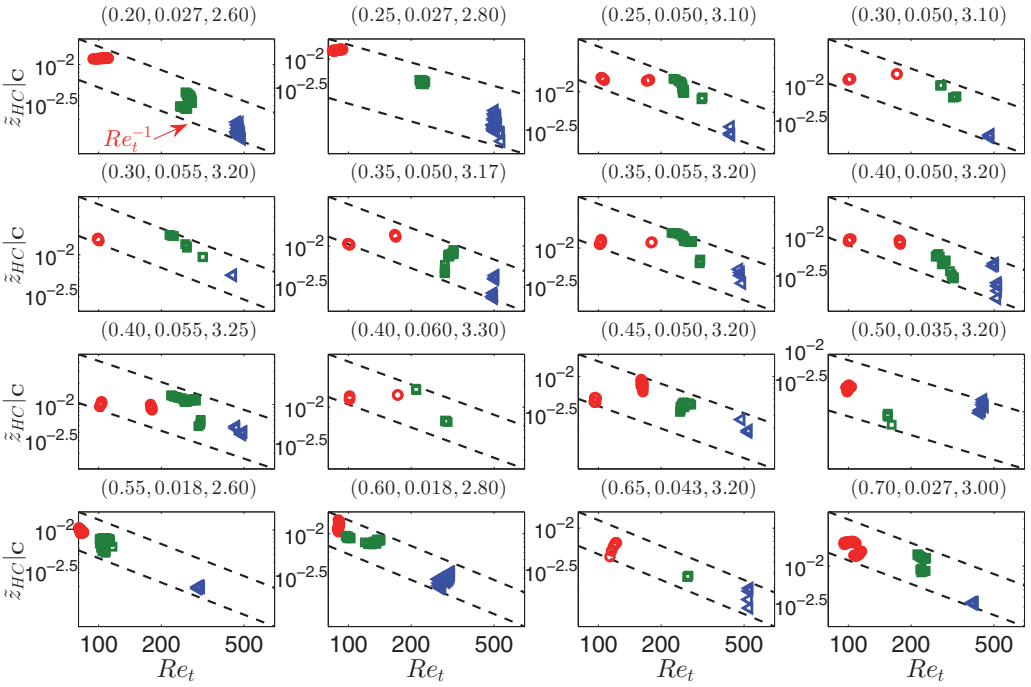

FIG. 4. Conditional average $\tilde{z}_{\mathrm{HC}}|_{\mathbf{C}}$ against Re_t in the three CO/H_2 DNS flames: case L, red circles; case M, green squares; and case H, blue triangles. The dashed lines are reference lines with slope -1 in the log-log plot. The condition $\mathbf{C}(c_m, c_r, c_\chi)$ for computing the conditional average $\tilde{z}_{\mathrm{HC}}|_{\mathbf{C}}$ is given above each plot.

used to balance these two considerations. Halving the values of these parameters yields a too small number of samples for the later probabilistic analysis. Doubling and tripling these parameters have been tried and they are found to have no significant effect on the results.

As argued in Sec. I, a local Reynolds number is needed to examine the DMD effect as a local phenomenon. Without using a local Reynolds number, Han *et al.* [27] reported a scaling factor for $z_{\mathrm{HC,rms}}$ ranging from $\mathrm{Re}_b^{-0.04}$ to $\mathrm{Re}_b^{-0.57}$ when the bulk Reynolds number Re_b was used in the analysis. In this work, we use the local turbulent Reynolds number defined in Eq. (4).

By using the local Reynolds number, we can obtain a large number of data points with a range of Re_t corresponding to the three DNS flames, while with the bulk Re_b only three points from the three flames can be obtained [27] for the Reynolds-number-scaling analysis for DMD.

B. Scaling results for conditional statistics

The obtained results for $\tilde{z}_{\mathrm{HC}}|_{\mathbf{C}}$ against Re_t are shown in Fig. 4 for the various conditions $\mathbf{C}$ ($0.2 < c_m < 0.7$, $0.018 < c_r < 0.060$, and $2.60 < c_\chi < 3.30$). The mean mixture fraction c_m in the range $[0.2, 0.7]$ is chosen so that we can focus on the DMD effect near the flame front where the mixture fraction is close to the stoichiometric value of 0.42. The mixture fraction rms c_r is specified to be within $[0.018, 0.060]$, which covers most of the global limit of the mixture fraction rms within $[0, 0.075]$ from all three DNS flames. The scalar dissipation rate c_χ is chosen to be within $[10^{2.60}\ \mathrm{s}^{-1}, 10^{3.30}\ \mathrm{s}^{-1}]$, which also covers a significant portion of the global limit within $[0, 10^{3.65}\ \mathrm{s}^{-1}]$. The low dissipation rate range (say, $c_\chi < 10^{2.6}\ \mathrm{s}^{-1}$) contains no sample data from the DNS flames when the ranges of the mixture fraction mean and rms have been specified. The range of the conditional sampling variables is expected to cover most relevant regions in the DNS flames where DMD is of interest. From Fig. 4 we can see that there is a clear trend of scaling Re_t^{-1} for the results of $\tilde{z}_{\mathrm{HC}}|_{\mathbf{C}}$ by comparing the DNS results with the reference lines (dashed lines) with deviation

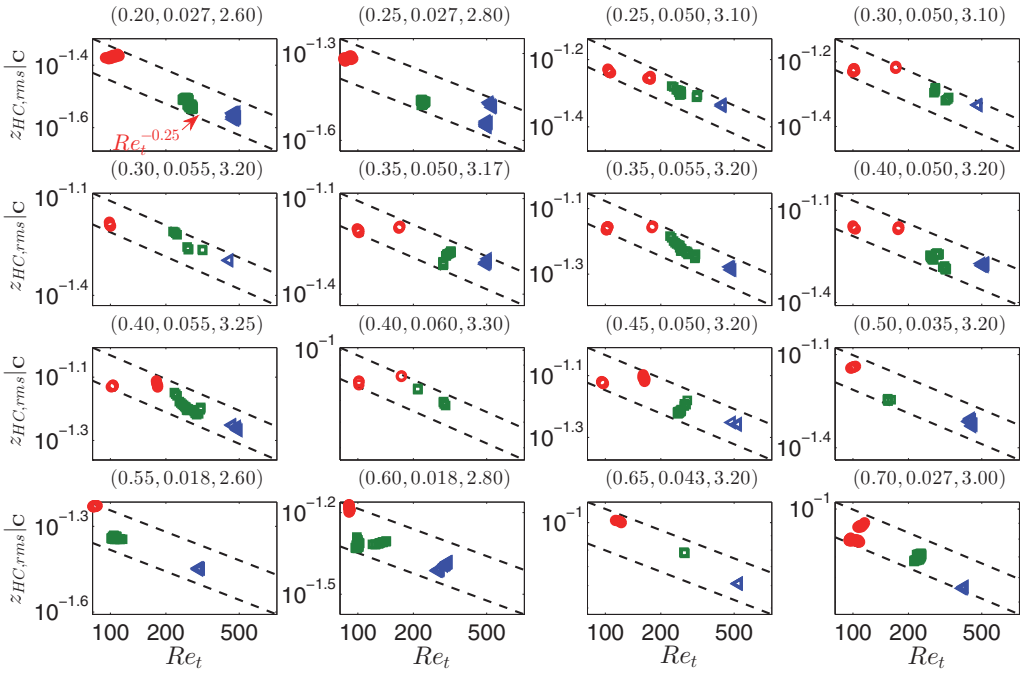

FIG. 5. Conditional average of $z_{\mathrm{HC,rms}}|_{\mathbf{C}}$ against Re_t in the three CO/H_2 DNS flames: case L, red circles; case M, green squares; and case H, blue triangles. The dashed lines are reference lines with slope -0.25 in the log-log plot. The condition $\mathbf{C}(c_m, c_r, c_\chi)$ for computing the conditional average $z_{\mathrm{HC,rms}}|_{\mathbf{C}}$ is given above each plot.

of some results from the scaling. This, to some extent, provides weak support to the scaling of Re_t^{-1} for $\tilde{z}_{\mathrm{HC}}$ obtained from the theoretical studies [4,28,38]. The exact scaling $\tilde{z}_{\mathrm{HC}} \sim \mathrm{Re}_t^{-1}$, however, is not seen in the Sandia DNS CO/H_2 flames.

The results for $z_{\mathrm{HC,rms}}|_{\mathbf{C}}$ against Re_t are shown in Fig. 5 from the three DNS flames. Similarly, a trend of the power-law scaling of $\mathrm{Re}_t^{-0.25}$ is seen from the results based on the comparison of the DNS results with the reference lines with slope -0.25 in the log-log plot, which supports the power-law scaling discussed in [28–30] to some extent. Deviation of some results from the scaling is also apparent.

C. Probabilistic analysis of power-law scaling exponents

The results in Figs. 4 and 5 provide some level of evidence to the power-law Reynolds-number scaling in the Sandia CO/H_2 DNS flames that is consistent with the literature results [28–30] but also show some evident deviation. To understand these scaling results more thoroughly, we next employ a probabilistic analysis of the scaling law for $\tilde{z}_{\mathrm{HC}}$ and $z_{\mathrm{HC,rms}}$ in the Sandia DNS flames. We assume a scaling of $\mathrm{Re}_t^{\kappa_m}$ for $\tilde{z}_{\mathrm{HC}}|_{\mathbf{C}}$ and $\mathrm{Re}_t^{\kappa_r}$ for $z_{\mathrm{HC,rms}}|_{\mathbf{C}}$ and write them as

$$\ln \tilde{z}_{\mathrm{HC}}|_{\mathbf{C}} \approx C_m + \kappa_m \ln \mathrm{Re}_t, \tag{9}$$

$$\ln z_{\mathrm{HC,rms}}|_{\mathbf{C}} \approx C_r + \kappa_r \ln \mathrm{Re}_t, \tag{10}$$

where C_m and C_r are parameters that are independent of Re_t, and κ_m and κ_r are the exponents for the power-law DMD scaling analysis. Based on the results in Figs. 4 and 5, we cannot find universal constants for κ_m and κ_r in the DNS flames. Thus, instead of trying to seek constants (e.g., $\kappa_m = -1$

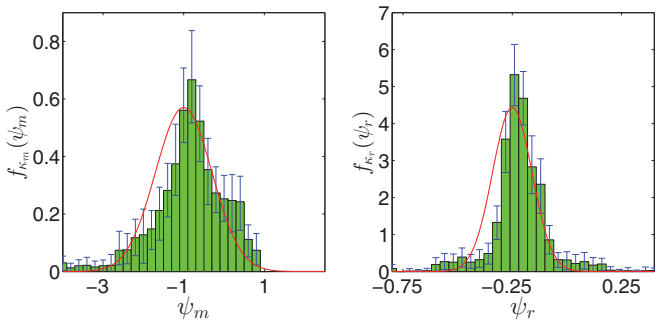

FIG. 6. The PDFs of scaling exponents κ_m (left) and κ_r (right). The solid lines are the Gaussian PDF with the mean and variance calculated from the data samples. The error bars are the estimated 95% confidence intervals.

and $\kappa_r = -0.25$) for a unique scaling of DMD, we view κ_m and κ_r as random variables. We aim to gain an understanding of the statistical distribution of κ_m and κ_r in the following analysis. The sample values of κ_m and κ_r can be obtained from the DNS results shown in Figs. 4 and 5. From Fig. 4, each pair of data points on the plots can be used to determine the values of C_m and κ_m by curving fitting using Eq. (9). We can use all different pairs of points in Fig. 4 to collect the statistical sample values of κ_m. The statistical samples of κ_r can be collected in the same way.

The PDF of κ_m and κ_r, $f_{\kappa_m}(\psi_m)$ and $f_{\kappa_r}(\psi_r)$, where ψ_m and ψ_r are the sample space variables corresponding to the random variables κ_m and κ_r, respectively, can then be approximated from the statistical samples of κ_m and κ_r, respectively. The bootstrap resampling method [39,40] is used to reduce the statistical error in the computed PDFs. The basic idea of the bootstrap resampling is to generate new sets of samples of κ_m and κ_r from the original data set for the estimation of the PDFs. The resampling is done by randomly selecting samples from the original data set with replacement to form a new set with equal sample size. This resampling can be repeated multiple times. Each data set (the original one or the new ones generated from resampling) can be used to compute the PDFs. The multiple PDFs computed from resampling can be averaged to form a PDF with a reduced statistical error. The standard deviation of the multiple PDFs can be calculated to estimate the 95% confidence interval to quantify the error in the estimation of the PDFs. Figure 6 shows the computed PDFs $f_{\kappa_m}(\psi_m)$ and $f_{\kappa_r}(\psi_r)$ with the estimated 95% confidence intervals. The bootstrap resampling is repeated 30 times for generating the PDFs in the figures. Both $f_{\kappa_m}(\psi_m)$ and $f_{\kappa_r}(\psi_r)$ show a Gaussian-like probability distribution. The PDF $f_{\kappa_m}(\psi_m)$ peaks at $\psi_m \approx -1$, and $f_{\kappa_r}(\psi_r)$ peaks at $\psi_r \approx -0.25$. This provides, in a statistical sense, a strong support to the DMD scaling $\tilde{z}_{\mathrm{HC}} \sim \mathrm{Re}_t^{-1}$ and $z_{\mathrm{HC,rms}} \sim \mathrm{Re}_t^{-0.25}$. These scaling can only be observed statistically, i.e., the probability of finding these scaling exponents is the highest when compared with other values. The statistical results of $\tilde{z}_{\mathrm{HC}} \sim \mathrm{Re}_t^{-1}$ are consistent with the theoretical results from the literature. The finding of $z_{\mathrm{HC,rms}} \sim \mathrm{Re}_t^{-0.25}$ supports those in [28–30]. The other scaling result $z_{\mathrm{HC,rms}} \sim \mathrm{Re}_t^{-1}$ [4] is not supported by the current findings, which confirms the speculation discussed in Sec. I (the scaling $z_{\mathrm{HC,rms}} \sim \mathrm{Re}_t^{-0.25}$ dominates the Re_t^{-1} scaling in real turbulence).

The exact scaling $\tilde{z}_{\mathrm{HC}} \sim \mathrm{Re}_t^{-1}$ and $z_{\mathrm{HC,rms}} \sim \mathrm{Re}_t^{-0.25}$ has a sound theoretical basis in idealized turbulence as discussed in Sec. I. The deviation from the theoretical scaling observed in the Sandia DNS flames requires some further examination. First of all, the theoretical scaling is expected only at a sufficiently high Reynolds number where a wide inertial range exists. Deviation from the theoretical scaling can be seen from a simple analysis of a mixing layer problem by Wang [5] when the Reynolds number is low. The examined DNS flames in this work covers only a small range of low to moderate Reynolds numbers. The relatively low Reynolds number is expected to be the main cause of the scattering of the DMD scaling exponents in Fig. 6. Hypothetically, the variance of the scaling exponents in Fig. 6 is inversely correlated with the Reynolds number. The higher the

Reynolds number, the smaller the variance. Examining this hypothesis, however, requires DNS cases with a wider range of Reynolds numbers, and it can be done when new DNS flames with different Reynolds number become available in the future. Second, the derivation of the theoretical scaling relies on an assumption of a turbulent energy spectrum, say, the Kolmogorov $-5/3$ energy spectrum. It is important to recognize that this spectrum can only be observed in a statistical sense even when the Reynolds number is sufficiently high. Locally and instantaneously, statistical fluctuations can cause the energy spectrum to deviate from the theoretical $-5/3$ scaling and hence pollute the theoretical scaling of DMD. This gives rise to a further scattering of the DMD scaling exponents in the currently examined DNS flames where the Reynolds numbers are not high enough. Third, the chemical reaction in turbulent combustion problems likely interferes with turbulence and molecular diffusion to cause the deviation of the DMD scaling from the theoretical results. The existence of a flame front in turbulent combustion can significantly affect the molecular diffusion process. The increase of temperature near a flame front can substantially increase the value of the molecular diffusivity and hence affects the molecular diffusion. The flame front can also affect the molecular diffusion by increasing the scalar gradient significantly if the flame front is thin. Additionally, the density change caused by chemical reaction can deviate turbulence from theoretical turbulence with constant density even if the Reynolds number is high. All these factors can cause the statistical distribution of the scaling exponents in Fig. 6. Finally, a number of assumptions are involved in the current probabilistic analysis of DMD in the Sandia DNS flames, including but not limited to the flamelet assumption in Eqs. (8) and (9) and neglecting the variation of local Da. These assumptions can likely contaminate the theoretical scaling as well. It is noted that although the global Da for all three DNS flames is the same, the contribution of Da to the scattering of the scaling exponents in Fig. 6 has likely been accounted for since the local Da in all three DNS flames is not a constant. Similar to the choice of the Reynolds number for the DMD scaling analysis, the local Da is a suitable choice for the examination of the dependence of the scaling exponents on the Da. Such dependence is not considered in the current analysis and hence its neglect is another plausible cause of the scattering of the scaling exponents observed in Fig. 6.

In summary, we conducted a thorough DMD scaling analysis in the Sandia CO/H_2 DNS flames. A plausible power-law Reynolds-number scaling in turbulent nonpremixed flames was reported. It was argued that it is more appropriate to interpret the DMD scaling with respect to the Reynolds number as a statistical result. These results support the theoretical findings obtained in simple and nonreacting flows. It can also explain why the DMD scaling is not evident in previous studies [27,31] if the analysis was not done statistically with a sufficient number of samples. These results are expected to be significant for guiding future development and validation of physical models for DMD that can yield the desired power-law Reynolds-number scaling [5]. In a separate work [41], we have attempted to investigate the turbulence modeling requirements to yields the observed power-law scaling of DMD.

IV. CONCLUSION

In this work, a scaling analysis of the effect of DMD with respect to the Reynolds number was performed in turbulent nonpremixed flames. A DNS data set of the Sandia CO/H_2 DNS flames was used to quantify the dependence of the effect of DMD on a local Reynolds number. A statistical analysis of this dependence showed that the effect of DMD on mean quantities has the highest probability of scaling Re_t^{-1} and the effect of DMD on rms quantities has the highest probability of scaling $\mathrm{Re}_t^{-0.25}$. A unique scaling, however, could not be observed in the DNS flames. These statistical scaling results are consistent, in a statistical sense, with previous findings from the theoretical analysis in nonreacting problems, indicating the insignificant effect of a chemical reaction on the scaling of DMD with respect to Reynolds number. This finding is important to guide future model development and simulations to be consistent with physical scaling laws.

ACKNOWLEDGMENTS

Acknowledgment is made of the Donors of the American Chemical Society Petroleum Research Fund (Grant No. 53781-DNI9) for support of this research. This paper was based upon work supported by the National Science Foundation under Grant No. CBET-1336075. This research was supported in part through computational resources provided by Information Technology at Purdue University, West Lafayette, Indiana.

[1] S. B. Pope, *Turbulent Flows* (Cambridge University Press, Cambridge, 2000).
[2] T. Poinsot and D. Veynante, *Theoretical and Numerical Combustion* (Edwards, Philadelphia, 2005).
[3] D. Veynante and L. Vervisch, Turbulent combustion modeling, Prog. Energy Combust. Sci. **28**, 193 (2002).
[4] W. Bilger and R. W. Dibble, Differential molecular diffusion effects in turbulent mixing, Combust. Sci. Technol. **28**, 161 (1982).
[5] H. Wang, Consistent flamelet modeling of differential molecular diffusion for turbulent non-premixed flames, Phys. Fluids **28**, 035102 (2016).
[6] T. Takagi, Y. Yoshikawa, K. Yoshida, M. Komiyama, and S. Kinoshita, Studies on strained non-premixed flames affected by flame curvature and preferential diffusion, Proc. Combust. Inst. **26**, 1103 (1996).
[7] D. C. Haworth and T. J. Poinsot, Numerical simulations of Lewis number effects in turbulent premixed flames, J. Fluid Mech. **244**, 405 (1992).
[8] D. H. Rowinski and S. B. Pope, Computational study of lean premixed turbulent flames using RANS/PDF and LES/PDF methods, Combust. Theory Model. **17**, 610 (2013).
[9] R. S. Barlow, M. J. Dunn, and G. Magnotti, Preferential transport effects in premixed bluff-body stabilized CH_4/H_2 flames, Combust. Flame **162**, 727 (2015).
[10] P. Cambray and G. Joulin, On moderately-forced premixed flames, Proc. Combust. Inst. **24**, 61 (1992).
[11] A. N. Lipatnikov and J. Chomiak, Molecular transport effects on turbulent flame propagation and structure, Prog. Energy Combust. Sci. **31**, 1 (2005).
[12] R. S. Barlow, J. H. Frank, A. N. Karpetis, and J.-Y. Chen, Piloted methane/air jet flames: Transport effects and aspects of scalar structure, Combust. Flame **143**, 433 (2005).
[13] H. Wang and K. Kim, Effect of molecular transport on PDF modeling of turbulent non-premixed flames, Proc. Combust. Inst. **35**, 1137 (2015).
[14] W. Han, V. Raman, and Z. Chen, LES/PDF modeling of autoignition in a lifted turbulent flame: Analysis of flame sensitivity to differential diffusion and scalar mixing time-scale, Combust. Flame **171**, 69 (2016).
[15] V. Gopalakrishnan and J. Abraham, Effects of multicomponent diffusion on predicted ignition characteristics of an n-heptane diffusion flame, Combust. Flame **136**, 557 (2004).
[16] D. Frederick and J. Y. Chen, Effects of differential diffusion on predicted autoignition delay times inspired by H_2/N_2 jet flames in a vitiated coflow using the linear eddy model, Flow Turbul. Combust. **93**, 283 (2014).
[17] A. Kronenburg and R. W. Bilger, Modelling differential diffusion in nonpremixed reacting turbulent flow: Application to turbulent jet flames, Combust. Sci. Technol. **166**, 175 (2001).
[18] A. Kronenburg and R. W. Bilger, Modelling differential diffusion in nonpremixed reacting turbulent flow: Model development, Combust. Sci. Technol. **166**, 195 (2001).
[19] M. Ma and C. B. Devaud, A conditional moment closure (CMC) formulation including differential diffusion applied to a non-premixed hydrogen-air flame, Combust. Flame **162**, 144 (2015).
[20] S. B. Pope, PDF methods for turbulent reactive flows, Prog. Energy Combust. Sci. **11**, 119 (1985).
[21] R. McDermott and S. B. Pope, A particle formulation for treating differential diffusion in filtered density function methods, J. Comput. Phys. **226**, 947 (2007).
[22] M. S. Anand and S. B. Pope, Diffusion behind a line source in grid turbulence, Turbul. Shear Flows **4**, 46 (1985).

[23] P. Zhang and H. Wang, Variance consistent mean shift particle model for treating differential molecular diffusion in transported PDF methods for turbulent reactive flows, Comput. Fluids **170**, 53 (2018).
[24] N. Peters, Laminar diffusion flamelet models in non-premixed turbulent combustion, Prog. Energy Combust. Sci. **10**, 319 (1984).
[25] H. Pitsch and N. Peters, A consistent flamelet formulation for non-premixed combustion considering differential diffusion effects, Combust. Flame **114**, 26 (1998).
[26] H. Pitsch, E. Riesmeier, and N. Peters, Unsteady flamelet modeling of soot formation in turbulent diffusion flames, Combust. Sci. Technol. **158**, 389 (2000).
[27] C. Han, D. O. Lignell, E. R. Hawkes, J. H. Chen, and H. Wang, Examination of the effect of differential molecular diffusion in DNS of turbulent non-premixed flames, Int. J. Hydrogen Energy **42**, 11879 (2017).
[28] A. R. Kerstein, M. A. Cremer, and P. A. McMurtry, Scaling properties of differential molecular diffusion effects in turbulence, Phys. Fluids **7**, 1999 (1995).
[29] V. Nilsen and G. Kosály, Differentially diffusing scalars in turbulence, Phys. Fluids **9**, 3386 (1997).
[30] M. Ulitsky, T. Vaithianathan, and L. R. Collins, A spectral study of differential diffusion of passive scalars in isotropic turbulence, J. Fluid Mech. **460**, 1 (2002).
[31] L. L. Smith, R. W. Dibble, L. Talbot, R. S. Barlow, and C. D. Carter, Laser Raman scattering measurements of differential molecular diffusion in turbulent nonpremixed jet flames of H_2/CO_2 fuel, Combust. Flame **100**, 153 (1995).
[32] L. Dialameh, M. J. Cleary, and A. Y. Klimenko, A multiple mapping conditioning model for differential diffusion, Phys. Fluids **26**, 025107 (2014).
[33] G. K. Batchelor, Small-scale variation of convected quantities like temperature in turbulent fluid part 1. General discussion and the case of small conductivity, J. Fluid Mech. **5**, 113 (1959).
[34] A. M. Oboukov, Structure of the temperature field in a turbulent flow, Izv. Akad. Nauk SSSR, Ser. Geogr. Geofiz. **13**, 58 (1949).
[35] E. R. Hawkes, R. Sankaran, J. C. Sutherland, and J. H. Chen, Scalar mixing in direct numerical simulations of temporally evolving plane jet flames with skeletal CO/H_2 kinetics, Proc. Combust. Inst. **31**, 1633 (2007).
[36] R. W. Bilger, S. H. Stårner, and R. J. Kee, On reduced mechanisms for methane air combustion in non-premixed flames, Combust. Flame **80**, 135 (1990).
[37] C. Bruno, V. Sankaran, H. Kolla, and J. H. Chen, Impact of multi-component diffusion in turbulent combustion using direct numerical simulations, Combust. Flame **162**, 4313 (2015).
[38] R. W. Bilger, Molecular transport effects in turbulent diffusion flames at moderate Reynolds number, AIAA J. **20**, 962 (1982).
[39] A. C. Davison and D. V. Hinkley, *Bootstrap Methods and Their Application* (Cambridge University Press, Cambridge, 1997), Vol. 1.
[40] P. Zhang, A. R. Masri, and H. Wang, Studies of the flow and turbulence fields in a turbulent pulsed jet flame using LES/PDF, Combust. Theory Model. **21**, 897 (2017).
[41] C. Han, T. Pant, U. Jain, and H. Wang, Consistent modeling of differential molecular diffusion to yield desired Reynolds-number power-law scaling, Phys. Fluids **30**, 085108 (2018).